

Complex self-assembled patterns using sparse commensurate templates with locally varying motifs

Joel K. W. Yang^{1†‡}, Yeon Sik Jung^{2†‡}, Jae-Byum Chang², R. A. Mickiewicz², A. Alexander-Katz², C. A. Ross^{2*} and Karl K. Berggren^{1*}

Templated self-assembly of block copolymer thin films can generate periodic arrays of microdomains within a sparse template, or complex patterns using 1:1 templates^{1–16}. However, arbitrary pattern generation directed by sparse templates remains elusive. Here, we show that an array of carefully spaced and shaped posts, prepared by electron-beam patterning of an inorganic resist, can be used to template complex patterns in a cylindrical-morphology block copolymer. We use two distinct methods: making the post spacing commensurate with the equilibrium periodicity of the polymer, which controls the orientation of the linear features, and making local changes to the shape or distribution of the posts, which direct the formation of bends, junctions and other aperiodic features in specific locations. The first of these methods permits linear patterns to be directed by a sparse template that occupies only a few percent of the area of the final self-assembled pattern, while the second method can be used to selectively and locally template complex linear patterns.

Microphase separation of a block copolymer thin film can generate dense arrays of microdomains with periodicity as low as ~ 10 nm (refs 6,16–19). Such arrays have been used as lithographic masks to pattern various functional materials, and to create devices including nanocrystal flash memory, nanowire transistors, gas sensors and patterned magnetic recording media^{20–25}. Block copolymer thin film self-assembly on an unpatterned substrate leads to close-packed arrays of features such as lines or dots that lack long-range order, thus limiting their utility. As a result, both chemical and topographical substrate features have been used to template or guide block copolymer self-assembly, imposing long-range order and generating microdomain geometries not observed in untemplated films^{1–16}. These templates are often defined using electron-beam lithography (EBL)^{3–5,7,8,11}, because of its ability to pattern small features of arbitrary geometry. However, the serial nature of EBL makes it clearly advantageous to minimize the density of the EBL-written features required to template a given arrangement of block copolymer microdomains. Even in a production context in which EBL is used only to write a master pattern that is to be replicated by some higher-throughput mechanism (such as nanoimprinting), the time required just to write the master can be prohibitively long. The challenge in template design is therefore to find a set of template features of minimum complexity that will deterministically program the block copolymer to form a desired final pattern, such as an interconnect level in an integrated circuit, which may contain both periodic and aperiodic features.

We describe an approach to this problem that uses a sparse array of chemically functionalized topographical posts to control the self-assembly of dense linear block copolymer (BCP) structures to form device-like nanopatterns. Most work on the templated self-assembly of block copolymers for nanolithography has focused on the generation of periodic patterns of parallel lines, close-packed dots or concentric rings, using shallow trenches^{1,6,9,10,12–14,22,24,26}, sparse post arrays³ or chemical templates with a periodicity either similar to that of the BCP^{2,7,8,15} or a factor two, three or four times larger^{3–5}. Nealey and colleagues have shown that non-regular features such as lamellae with bends^{2,11} or square-packed dots¹⁵ could be formed using a chemical pattern of the same density as the desired block copolymer pattern. Meanwhile, Cheng and colleagues have used discontinuous chemical lines to direct the locations of lamellae⁴. In contrast, the work described here uses sparse arrays of posts to both control the in-plane orientation of linear features, according to the commensurability between the post lattice and block copolymer period, and also to create specific non-regular features by locally modifying the post shape and spacing into an arrangement that changes the preferred commensuration condition, resulting in a linear connected pattern that can be routed selectively to form complex bent structures and junctions. This pattern may be particularly useful in microelectronic device fabrication to form, for example, interconnect levels in which the posts are designed to be incorporated into the final desired device layout.

This concept is demonstrated using a polystyrene-*b*-polydimethylsiloxane (PS-*b*-PDMS) block copolymer with molecular weight $M_w = 45.5$ kg mol⁻¹ and minority-block volume fraction $f_{PDMS} = 33.5\%$, which microphase-separates to form PDMS cylinders within a PS matrix. Spin-coating a film of the block copolymer onto a smooth substrate, then solvent-annealing and etching^{25–27} (see Supplementary Information for methods) yields oxidized PDMS cylinders with a natural period L_o of ~ 35 nm and with varying in-plane orientations as shown in Fig. 1. Figure 1a schematically illustrates the templating process. A rectangular array of posts with heights of ~ 35 nm and diameters of ~ 10 nm was fabricated on the substrate by means of EBL exposure of hydrogen silsesquioxane (HSQ) resist^{3,28}. The HSQ posts and native oxide on the silicon wafers were chemically functionalized with a brush layer of PDMS to ensure that the posts had an affinity for the PDMS block of the block copolymer and to improve annealing kinetics. Thin PDMS layers formed at the air and substrate interfaces^{3,25–27}.

We first demonstrate that the order and orientation of the block copolymer cylinders (with equilibrium period L_o) can be

¹Department of Electrical Engineering and Computer Science, Massachusetts Institute of Technology, 77 Massachusetts Avenue, Cambridge, Massachusetts 02139, USA; ²Department of Materials Science and Engineering, Massachusetts Institute of Technology, 77 Massachusetts Avenue, Cambridge, Massachusetts 02139, USA; [†]Present address: Institute of Materials Research and Engineering, 3 Research Link, Singapore 117602 (J.K.W.Y.); Department of Materials Science and Engineering, Korea Advanced Institute of Science and Technology, 335 Gwahangno, Yuseong-gu, Daejeon, 305-701, Republic of Korea (Y.S.J.); [‡]These authors contributed equally to this work. *e-mail: caross@mit.edu; berggren@mit.edu

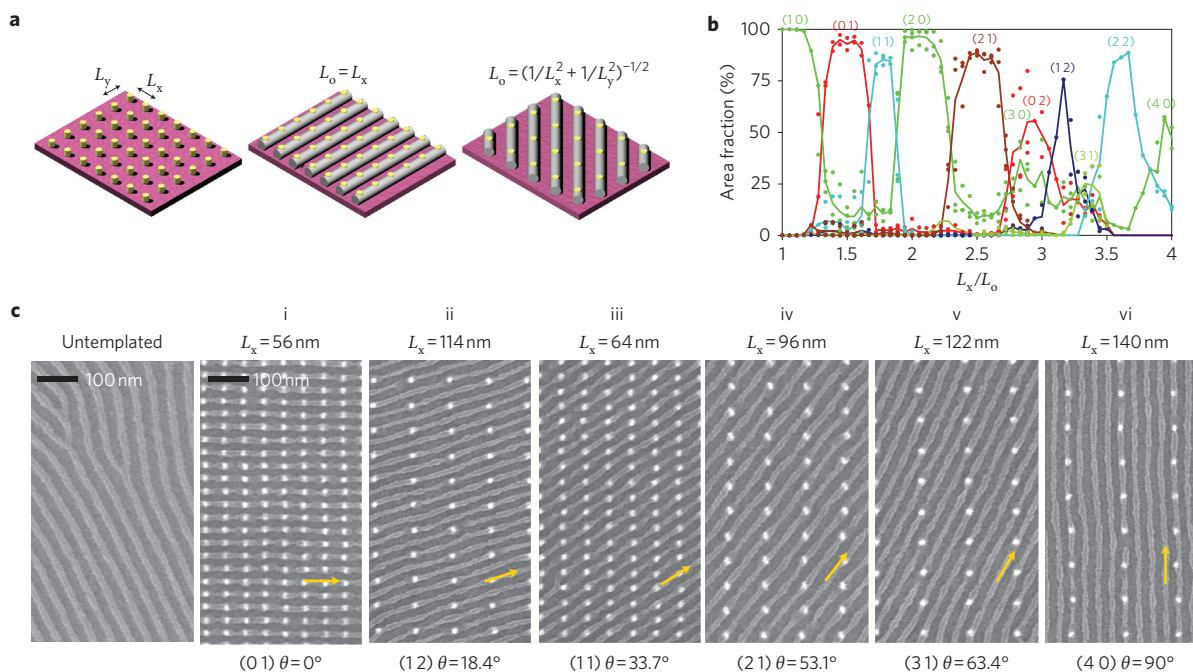


Figure 1 | Commensurate templating of a cylindrical morphology PS-PDMS block copolymer. **a**, Left: schematic showing a simplified view of the template consisting of HSQ nanoposts (yellow) on a silicon substrate (pink). Centre: when $L_0 = L_x$, the PDMS cylinders self-assemble parallel to the y -axis to satisfy commensuration, forming a (0 1) lattice. Right: when $L_0 = (1/L_x^2 + 1/L_y^2)^{-1/2}$, the cylinders align diagonally with respect to the template lattice to maintain their equilibrium spacing, forming a (1 1) lattice. **b**, Plot of area fraction of each lattice versus L_x/L_0 for templates with a range of L_x of 30–150 nm. $L_x/L_0 = 1.6$ corresponds to the sample of Fig. 1c(i). For orientations other than $(i\ 0)$ the area fractions shown here represent a slight underestimate of the actual area fraction as a result of an image analysis artifact (discussed in the Supplementary Information). **c**, SEM images of an untemplated monolayer of cylindrical PDMS domains on a flat surface after selective etching to remove the PDMS surface layer and the PS matrix. Panels i–vi show several commensurate $(i\ j)$ cylinder lattices formed on templates where $L_x/L_y = 1.5$. The arrows indicate the direction of the BCP cylinders, which makes an angle θ with the x -axis of the template.

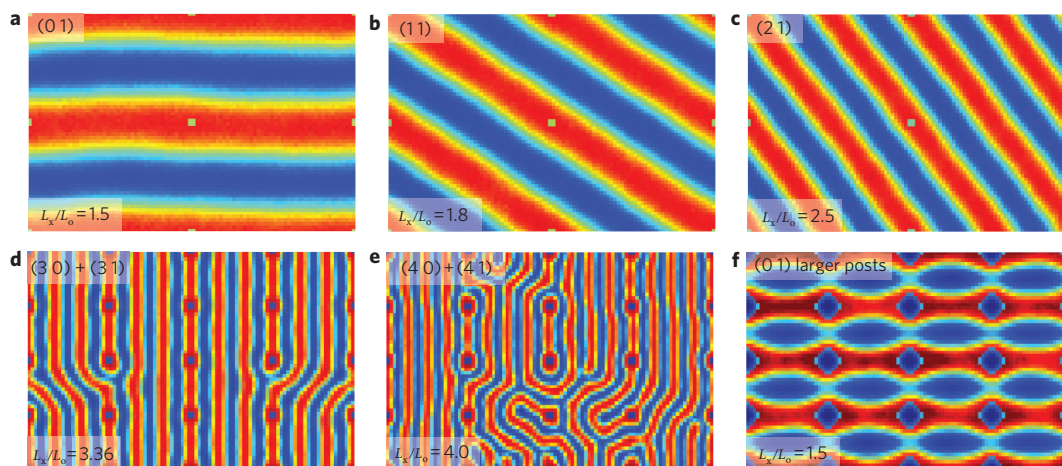


Figure 2 | Modelling of block copolymer microdomain morphologies. **a–f**, The plots show the density distribution of the A block of an AB diblock copolymer self-assembled on a post array with $L_x/L_y = 1.5$. The posts attract the A block (red). The spacing between posts (blue dots) was varied to guide the orientation of the microdomains. L_x/L_0 increased from 1.5 (**a**) to 1.8 (**b**), 2.5 (**c**), 3.36 (**d**) and 4.0 (**e**), inducing a change in the orientation from (0 1) to (1 1), (2 1), (3 1) and (4 0), respectively. In **d**, a mixture of (3 1) and (3 0) orientations formed. In **e**, (4 0) and (4 1) orientations formed. In **f**, the (0 1) orientation formed, even when the post diameter was increased.

programmed using a rectangular lattice of posts with lattice parameters L_x and L_y by considering the commensuration condition between L_0 , L_x and L_y (Fig. 1a; see also Supplementary Fig. S1). In the case when $L_0 = L_x$, the cylinders orient along the y -axis. However, for a larger L_x , such that $L_0 = (1/L_x^2 + 1/L_y^2)^{-1/2}$, the PDMS cylinders align diagonally along the [1 1] direction of the post lattice. These commensurate orientations are designated (1 0)

and (1 1), respectively, by analogy to the two-dimensional Miller indexing of crystal lattice planes. By varying the lattice parameters L_x and L_y , one can achieve a broad range of block copolymer lattice orientation angles (Supplementary Fig. S1C). The plot in Supplementary Fig. S1C shows the calculated commensurate condition for a generic rectangular template with $L_x = \alpha L_y$, where the microdomain array has period $L_0 < L_x$. Commensuration for

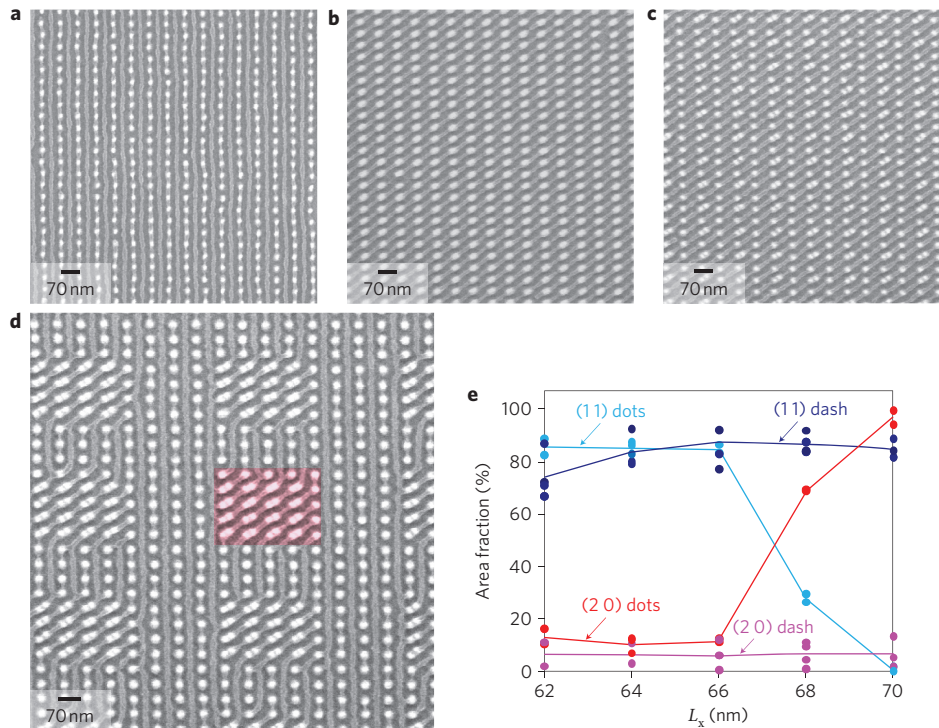


Figure 3 | Demonstration of local programming of the block copolymer arrangement by changing the motif of the template lattice. SEM images of different template motifs with the same L_x spacing of 70 nm and $L_x/L_y = 1.5$. **a**, As expected, the block copolymer with a natural period of $L_o = 35$ nm formed an unstrained commensurate lattice of vertical lines in the (2 0) direction on a template consisting of single circular posts. This orientation was also expected to switch from vertical lines (2 0) to diagonal lines (1 1) as L_x was decreased from 70 to 63 nm. **b**, Without changing L_x , but by simply changing the template motif from circular posts to diagonal dashes, the block copolymer lattice was made to align to the (1 1) orientation. This switch in orientation occurred despite significant strain in the block copolymer lattice by 11% as the block copolymer period increased from 35 to 38.8 nm. **c**, The same result as in **b** can be obtained by using a sparse array of double-post structures distributed among single posts. **d**, When the double-post structures were localized instead of distributed, we obtained a template that programmed regions of diagonal-line arrays (one region is colourized) surrounded by regions of vertical lines. **e**, Quantitative analysis showing the prevalence of the (1 1) and (2 0) lattices as a function of L_x . Using circular posts, the block copolymer lattice switched from (1 1) to (2 0) when L_x increased from 62 to 70 nm. However, with the dash (or double-post) motif, the (1 1) orientation was made to form preferably over the entire range of L_x shown.

lattice ($i j$) occurs when $L_x/L_o = \sqrt{[i^2 + (\alpha j)^2]}$, and the angle between the cylindrical microdomains and the x -axis is given by $\theta = \pm \text{atan}(i/\alpha j)$ (only positive angles are shown in Supplementary Fig. S1C). Degenerate cylinder lattices can occur at angles of $\pm \theta$, unless $\theta = 0^\circ$ or 90° .

Figure 1c(i–vi) gives examples of self-assembly on post arrays with various L_x values for the specific case of templates where $L_x = 1.5L_y$. Experimentally, L_x was varied from 30 to 140 nm in steps of 2 nm; the area coverage of each lattice orientation is plotted against L_x/L_o in Fig. 1b, maintaining the $L_x = 1.5L_y$ condition. This result is discussed in more detail in the Supplementary Information, but for now we note simply that the observed dominant lattice types agree with those predicted from the commensurability conditions and energy landscape presented in Supplementary Fig. S3B. This result is in close analogy with previous results on templating of close-packed arrays of spherical microdomains³.

To gain further insight into the self-assembly, we used a self-consistent field theory (SCFT)^{29,30} to compute the equilibrium morphologies of the corresponding two-dimensional lamellar system and compared them with the experimental results (Supplementary Section S6). The simulations were performed on a 96×64 rectangular lattice, with $\chi N = 13$ (χ is the Flory–Huggins interaction parameter and N the degree of polymerization) and a volume fraction $f = 0.5$. This volume fraction was chosen to represent the in-plane cylinders as vertical lamellae in the two-dimensional model. Figure 2 shows the results for L_x/L_o between 1.5 and 3.36, where $L_x = 1.5L_y$. The microdomain orientations that form match those found experimentally, as predicted from the commensurability

condition. For $L_x/L_o = 3.36$, the model generated a pattern containing both the commensurate (3 0) and strained (3 1) lattices, which differ by only $\sim 10\%$ in period. Similarly, multiple orientations were often observed for higher values of L_x/L_o (Fig. 2e). A lamellar structure would be expected to accommodate larger changes in its equilibrium spacing than a cylindrical one, promoting the formation of multiple lattices in the model. Nevertheless, annealing of the present simulations by introducing fluctuations that are present in the real system is expected to lower the defect levels seen in simulations such as in Fig. 2e. The model also showed that the self-assembly is insensitive to post size (Fig. 2f; see also Supplementary Fig. S4) and to χN in the range 12–15 (data not shown).

More complex block copolymer patterns can be produced by varying the post lattice geometry and also its motif. For example, if a set of posts is replaced by a set of dashes or pairs of closely spaced dots, the PDMS cylinders preferentially align parallel to the dashes, even if this new orientation has a periodicity that is further from the equilibrium spacing L_o than other possible orientations. This alignment parallel to the dashes is assumed to occur so as to minimize the distortion of the cylindrical shape of the microdomains caused by the posts. Varying the placement of the dashes can thus lead to bends, jogs or junctions in well-defined locations. Figure 3 shows how changes in the post lattice motif led to the formation of a (1 1) cylinder array even though the (2 0) array had a lower strain. In this example, $L_x = 70$ nm $= 2L_o$, so the unstrained (2 0) array was expected to form in a lattice with circular posts (Fig. 3a). However, replacing the circular posts with dashes (Fig. 3b) or double dots (Fig. 3c) led to the formation of a (1 1) array, despite its lattice

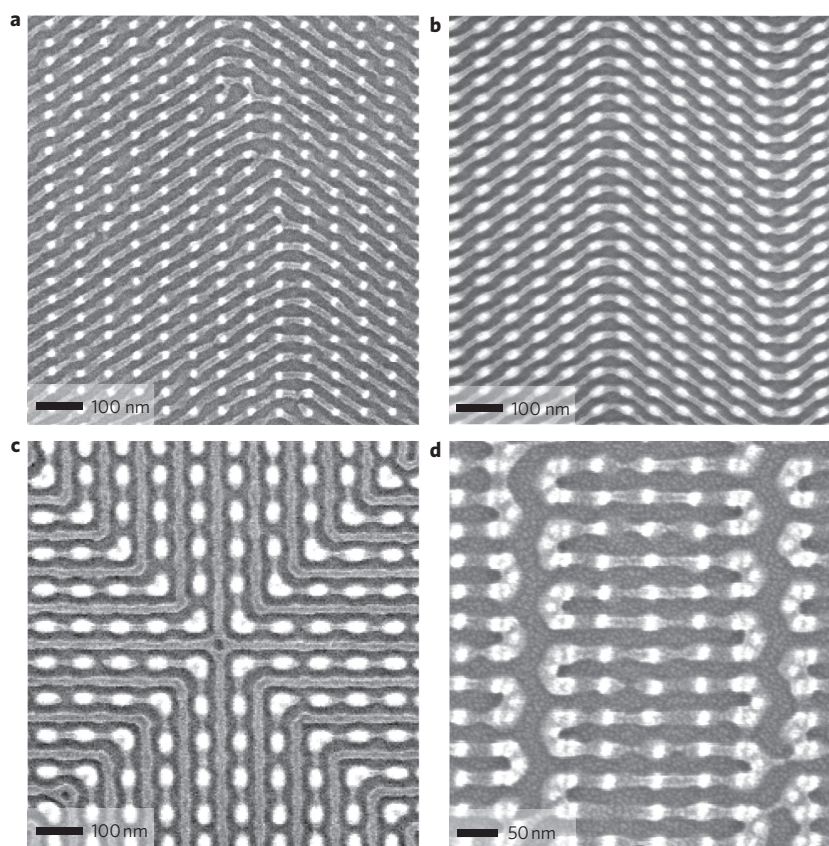


Figure 4 | Templated bends and junctions. **a**, Using a template consisting of a rectangular lattice of circular posts, bends form in random locations as the block copolymer cylinder lattice changes between degenerate variants, in this case (1 1) and $(\bar{1} 1)$. For circular posts there was no preference for one variant over another, and defects formed at random locations where one variant switched to another. **b**, By using an array of dashes instead of circular posts, the degeneracy can be broken to achieve a zig-zag pattern with bends at designated positions. **c**, Similarly, by using an array of dashes oriented in the x - and y -directions, nested-elbow structures form with a cross-point junction in the centre. **d**, The addition of posts at strategic locations can define a meander structure with sharp bends. In this example, the spacing between adjacent meanders was too large, and defects form where PDMS lines bridge between meanders.

expansion of 11% relative to the equilibrium period of $L_o = 35$ nm. By locally manipulating the template (Fig. 3d, double-dot regions), one can direct the block copolymer to form a strained lattice that remains commensurate with the underlying template, but oriented differently from the unstrained commensurate orientation. Figure 3e shows quantitatively that the dash or double-dot posts extend the range of post period over which the (1 1) cylinder orientation dominates.

A local motif can also be used to select between two energetically equivalent (that is, degenerate) lattices that would otherwise compete randomly in a post lattice. This method can be used to template a variety of more complex structures that have the potential for use in integrated circuit interconnects. Figure 4a shows an example of a lattice consisting only of dots where a degeneracy occurs between the $\theta = +33.7^\circ$ (1 1) and -33.7° ($\bar{1} 1$) cylinder lattices. Both orientations occupy almost equal areas of the post template, and bends have formed at random locations where one orientation has switched to the other. However, bends and junctions can be controlled to form at desired positions by making one orientation more energetically favourable than the other, using posts in the shape of dashes. Using this method, we created 'zig-zag' structures (Fig. 4b) and a single cross-point with surrounding nested-elbow structures (Fig. 4c).

We have so far shown that the BCP microdomains can be bent by up to 90° to form jogs, zig-zags and cross-points. Satisfying the commensuration condition and changing the motif of the posts were effective approaches to achieving these results. We have also observed that placing additional guiding posts in the template can introduce further complexity. For example, Fig. 4d shows that a single cylindrical microdomain can be folded into a tight meander structure by

positioning three additional posts at each bend. The underlying rectangular pattern to which these posts were added was identical to that in Fig. 1c(i), so it is clear that the additional posts reorient the microdomain morphology from a grating into a meander structure.

These results and discussions thus demonstrate two specific and distinct techniques for the formation of arrays of lines containing complex structures. In the first technique, the post period must be selected with an appropriate commensurate condition so as to determine the overall in-plane direction of the cylinders. In our experiments, well-ordered cylinders formed over hundreds of nanometre- or micrometre-sized areas up to at least $L_x/L_o = 4$, the largest spacing investigated. Lines of any orientation may be templated by choosing an appropriate value of L_x/L_y and L_x/L_o ratios. For example, templates that preserve L_y while varying L_x across the substrate would result in the formation of a pattern with spatially varying orientation, analogous to the results presented in Fig. 1c. As L_x/L_o increases, there is an increasing tendency to form multiple lattice types with similar period, implying a compromise between the post density and the defect levels in the self-assembled structure. However, the formation of multiple lattice types and variants can be suppressed by using the second technique presented in this paper: making at least some of the posts in the shape of dashes, as in Fig. 3c, and adding guiding posts, as in Fig. 4d. Local aperiodic features are then introduced by changing the period or motif of the lattice or by adding guiding posts in a manner suggested by Fig. 4.

The templating approach presented above can be used for patterning a range of useful structures. For example, to pattern electrical interconnects, one would need to design a template that links a single microdomain between a series of designated points. Regions

where no interconnects are desired may be defined by forming the linear features into closed paths, which will be electrically isolated. The final complex patterns can then be transferred into metal using previously demonstrated techniques²⁷.

The major advantage of this templated self-assembly technique is that the post array requires much less time to write than the entire layout. In the (4 0) lattice, for example (Fig. 1c(vi)), a well-ordered array of lines was templated by posts that occupied less than 3% of the area occupied by the lines, giving a factor of 37 increase in throughput compared to patterning the entire area of the linear features using EBL. Additionally, the edge roughness of the features (typically 3–4 nm r.m.s. roughness based on scanning electron microscopy (SEM) images of block copolymers self-assembled in trenches without posts) is determined primarily by the χ -parameter of the block copolymer. We believe that the edge roughness can be further reduced by optimizing the post dimensions (to minimize distortion of the cylinders) and the etch process. The process is expected to be scalable to smaller features; for example, a similar block copolymer of 16 kg mol⁻¹ forms well-ordered linear features with a period of 17 nm and linewidth of 8 nm.

In summary, the templated self-assembly method described here provides a way to define dense linear patterns with well-defined geometry at high throughput, using a sparse template that determines the in-plane orientation of the block copolymer microdomain array, and directs the formation of non-periodic structures. This process can decrease the patterning time required for making pattern masters by a factor of 30 or more when compared to the use of electron-beam lithography alone. Ultimately, it is expected that arbitrary structures such as interconnect layouts can be patterned using a template design that contains the minimum necessary information (that is, guiding features) to program the formation of a unique block copolymer pattern.

Received 18 August 2009; accepted 1 February 2010;
published online 14 March 2010

References

- Bang, J., Jeong, U., Ryu, D. Y., Russell, T. P. & Hawker, C. J. Block copolymer nanolithography: translation of molecular level control to nanoscale patterns. *Adv. Mater.* **21**, 1–24 (2009).
- Stoykovich, M. P. *et al.* Directed assembly of block copolymer blends into nonregular device-oriented structures. *Science* **308**, 1442–1446 (2005).
- Bitá, I. *et al.* Graphoepitaxy of self-assembled block copolymers on 2D periodic patterned templates. *Science* **321**, 939–943 (2008).
- Cheng, J. Y., Rettner, C. T., Sanders, D. P., Kim, H. C. & Hinsberg, W. D. Dense self-assembly on sparse chemical patterns: rectifying and multiplying lithographic patterns using block copolymers. *Adv. Mater.* **20**, 3155–3158 (2008).
- Ruiz, R. *et al.* Density multiplication and improved lithography by directed block copolymer assembly. *Science* **321**, 936–939 (2008).
- Park, S. *et al.* Macroscopic 10-terabit-per-square-inch arrays from block copolymers with lateral order. *Science* **323**, 1030–1033 (2009).
- Kim, S. O. *et al.* Epitaxial self-assembly of block copolymers on lithographically defined nanopatterned substrates. *Nature* **424**, 411–414 (2003).
- Wilmes, G. M., Durkee, D. A., Balsara, N. P. & Liddle, J. A. Bending soft block copolymer nanostructures by lithographically directed assembly. *Macromolecules* **39**, 2435–2437 (2006).
- Segalman, R. A., Hexemer, A. & Kramer, E. J. Edge effects on the order and freezing of a 2D array of block copolymer spheres. *Phys. Rev. Lett.* **91**, 192101 (2003).
- Segalman, R. A., Yokoyama, H. & Kramer, E. J. Graphoepitaxy of spherical domain block copolymer films. *Adv. Mater.* **13**, 1152–1155 (2001).
- Stoykovich, M. P. *et al.* Directed self-assembly of block copolymers for nanolithography: fabrication of isolated features and essential integrated circuit geometries. *ACS Nano* **1**, 168–175 (2007).
- Sundrani, D., Darling, S. B. & Sibener, S. J. Guiding polymers to perfection: macroscopic alignment of nanoscale domains. *Nano Lett.* **4**, 273–276 (2004).
- Black, C. T. & Bezencenet, O. Nanometer-scale pattern registration and alignment by directed diblock copolymer self-assembly. *IEEE Trans. Nanotechnol.* **3**, 412–415 (2004).
- Cheng, J. Y., Mayes, A. M. & Ross, C. A. Nanostructure engineering by templated self-assembly of block copolymers. *Nature Mater.* **3**, 823–828 (2004).
- Park, S. M., Craig, G. S. W., La, Y. H., Solak, H. H. & Nealey, P. F. Square arrays of vertical cylinders of PS-*b*-PMMA on chemically nanopatterned surfaces. *Macromolecules* **40**, 5084–5094 (2007).
- Bates, F. S. & Fredrickson, G. H. Block copolymer thermodynamics—theory and experiment. *Annu. Rev. Phys. Chem.* **41**, 525–557 (1990).
- Park, M., Harrison, C., Chaikin, P. M., Register, R. A. & Adamson, D. H. Block copolymer lithography: periodic arrays of $\sim 10^{11}$ holes in 1 square centimeter. *Science* **276**, 1401–1404 (1997).
- Tang, C. B., Lennon, E. M., Fredrickson, G. H., Kramer, E. J. & Hawker, C. J. Evolution of block copolymer lithography to highly ordered square arrays. *Science* **322**, 429–432 (2008).
- Bang, J. *et al.* Defect-free nanoporous thin films from ABC triblock copolymers. *J. Am. Chem. Soc.* **128**, 7622–7629 (2006).
- Milliron, D. J., Raoux, S., Shelby, R. & Jordan-Sweet, J. Solution-phase deposition and nanopatterning of GeSbSe phase-change materials. *Nature Mater.* **6**, 352–356 (2007).
- Cheng, J. Y., Jung, W. & Ross, C. A. Magnetic nanostructures from block copolymer lithography: hysteresis, thermal stability and magnetoresistance. *Phys. Rev. B* **70**, 064417 (2004).
- Black, C. T. Self-aligned self assembly of multi-nanowire silicon field effect transistors. *Appl. Phys. Lett.* **87**, 163116 (2005).
- Thurn-Albrecht, T. *et al.* Ultrahigh-density nanowire arrays grown in self-assembled diblock copolymer templates. *Science* **290**, 2126–2129 (2000).
- Naito, K., Hieda, H., Sakurai, M., Kamata, Y. & Asakawa, K. 2.5-inch disk patterned media prepared by an artificially assisted self-assembling method. *IEEE Trans. Magn.* **38**, 1949–1951 (2002).
- Jung, Y. S., Jung, W., Tuller, H. L. & Ross, C. A. Nanowire conductive polymer gas sensor patterned using self-assembled block copolymer lithography. *Nano Lett.* **8**, 3776–3780 (2008).
- Jung, Y. S. & Ross, C. A. Orientation-controlled self-assembled nanolithography using a polystyrene-polydimethylsiloxane block copolymer. *Nano Lett.* **7**, 2046–2050 (2007).
- Jung, Y. S., Jung, W. & Ross, C. A. Nanofabricated concentric ring structures by templated self-assembly of a diblock copolymer. *Nano Lett.* **8**, 2975–2981 (2008).
- Yang, J. K. W. & Berggren, K. K. Using high-contrast salty development of hydrogen silsesquioxane for sub-10-nm half-pitch lithography. *J. Vac. Sci. Technol. B* **25**, 2025–2029 (2007).
- Fredrickson, G. H. *The Equilibrium Theory of Inhomogeneous Polymers* (Oxford Univ. Press, 2006).
- Fredrickson, G. H., Ganesan, V. & Drolet, F. Field-theoretic computer simulation methods for polymers and complex fluids. *Macromolecules* **35**, 16–39 (2002).

Acknowledgements

The authors acknowledge support from the Semiconductor Research Corporation, the Singapore-MIT Alliance, the Office of Naval Research, and the Nanoelectronics Research Institute. J.K.W.Y. would like to acknowledge his fellowship from A*STAR Singapore. The Research Laboratory of Electronics Scanning-Electron-Beam Lithography Facility provided facilities for this work. The authors also thank M. Mondol and J. Daley for technical assistance and acknowledge helpful discussions with E.L. Thomas.

Author contributions

J.K.W.Y., Y.-S.J., C.A.R. and K.K.B. conceived and designed the experiments. J.K.W.Y., Y.-S.J. and J.B.C. analysed the experimental results. Y.-S.J. developed the analytical model. R.A.M. and A.A.-K. performed numerical modelling. All authors contributed to discussions and writing of the paper.

Additional information

The authors declare no competing financial interests. Supplementary information accompanies this paper at www.nature.com/naturenanotechnology. Reprints and permission information is available online at <http://npg.nature.com/reprintsandpermissions/>. Correspondence and requests for materials should be addressed to C.A.R. and K.K.B.